Sensors & Transducers, Vol. 168, Issue 4, April 2014, pp. 127-132

Sensors & Transducers

A Novel Approach for Analyzing Water Diffusion in Mineral and Vegetable Oil-Paper Insulation

Bin Du, * Jian Li, Zhaotao Zhang
State Key Laboratory of Power Equipment & System Security and New Technology
College of Electrical Engineering
Chongqing University, Chongqing, 400044, China
* Tel.: +86 23 65106880, fax: +86 23 65102442
* E-mail: lijian@cqu.edu.cn

Received: 14 February 2014 /Accepted: 14 March 2014 /Published: 30 April 2014

Abstract: Water diffusion characteristics of mineral and vegetable oil-paper insulation systems are important for insulation condition evaluation of oil-filled transformers. In this paper, we describe a novel application method of in situ attenuated total reflection Fourier transform infrared (ATR-FTIR) approach for analyzing the diffusion process of water molecules in oil-immersed insulating paper. Two-dimensional correlation was used to analyze the 3700 cm^{-1} to 3000 cm^{-1} hydroxyl peak. The observed results indicated that water molecules form two types of hydroxyl (OH) with oil-impregnated paper in the diffusion process are weak and strong hydrogen bonds, respectively. 2D infrared correlation analysis revealed that three OH stretching vibration spectra absorption peaks was existed in hygroscopic vegetable oil-immersed insulating paper. And there are four OH stretching vibration spectra absorption peaks in mineral oil-immersed insulation paper. Furthermore, mineral oil-impregnated paper and vegetable oil-impregnated paper diffusion coefficients were obtained by nonlinear fitting. *Copyright © 2014 IFSA Publishing, S. L.*

Keywords: ATR-FTIR, Oil-paper insulation, Water diffusion, Diffusion coefficient.

1. Introduction

Insulation paper, pressboard, and insulating oils are major insulation materials in oil-filled power transformers. These materials should be maintained under virtually dry conditions for their entire lives to ensure good insulation and safe operation of the oil-filled power transformers. An automatic Coulometric Karl Fischer Titration approach to determine water contents in insulating liquids, oil-impregnated paper and pressboard was presented in the IEC standard 60814-1997 [1]. However, water content in oil-impregnated paper and pressboard is difficult to be measured after oil-filled transformers are put into operation [2]. Dew point method was also used to measure the water contents of oil-paper insulation. The main disadvantage of the dew point method is that high requirements for equipment.

This work was motivated by two problems posed in the aforementioned publications for future applications. First, these methods in the above publications only measure the water content of the oil-paper insulation and cannot reflect the water molecular diffusion process in the oil-paper insulation. Secondly, the water diffusion characteristics in vegetable oil-paper insulations have seldom been investigated although vegetable insulating oils are used in medium-voltage transformers [8]. The moisture saturation level of vegetable insulating oils is greater than that

of mineral insulating oils, because the hydrophilic bonds exist in the ester molecules [9, 10]. The water diffusion characteristics of vegetable oil-paper insulations are thus different from those of mineral oil-paper insulations.

The paper shows an experiment system to simulate water diffusion in vegetable and mineral oil-paper and present a novel approach of two dimensional/attenuated total reflection (2D ATR) infrared correlation spectroscopic analysis of water diffusion in mineral and vegetable oil-paper insulation. The correlation analysis of the 2D ATR technology is an effective method of studying the water diffusion process at molecular level. The 2D ATR technology does not only improve the spectral resolution, but also provides dynamic information over the sequence of functional groups. Based on Fick's second law, the curves is deduced to simulate the water diffusion characteristics in mineral and vegetable oil-paper insulation. The water diffusion curves between vegetable and mineral oil-paper insulations are also compared.

2. Experiment

2.1. Preparation of Materials and Samples

A type of conventional naphthenic-based mineral insulating oil and a type of rapeseed insulating oil were used in the experiment. The paper used for the experiment was an ordinary, 0.3 mm thick insulating Kraft paper. The insulating paper specimens were dried in a vacuum vessel at 50 Pa and 90 °C for 48 hours to decrease the water content of each paper specimen to less than 0.5 %. The insulating oils were dried at 85 °C in a vacuum vessel for 48 hours to lower the water content of oil sufficiently. After the insulating specimens were prepared, the paper specimens were impregnated in the degassed and dried insulating oil at 40 °C under a vacuum for 24 hours. Finally, the oil-impregnated paper specimens were moved into the well-sealed glass bottle for use.

2.2. Diffusion Experiments

All infrared spectra for the water diffusion were performed at 25 °C using a Nicolet Nexus Smart ARK-FTIR spectrometer equipped with a DTGS-KBr detector, solid cell accessories, and a ZnSe IRE crystal. Before each experiment, the crystals were cleaned by washing with acetone and were dried under the infrared lamp. A 0.3 mm thick oil-impregnated paper was sandwiched between the ZnSe reflection elements. The filter paper and was mounted in the ATR cell, as shown in Fig. 1. The spectrum of the dry film was collected as the background spectra. Distilled water was injected into the filter paper, while the data acquisition was performed at 1 min intervals. Spectra were obtained between 4,000 cm^{-1} – 650 cm^{-1} at a resolution of 4 cm^{-1}. All of the original spectra were baseline-corrected using Omnic 8.1 software.

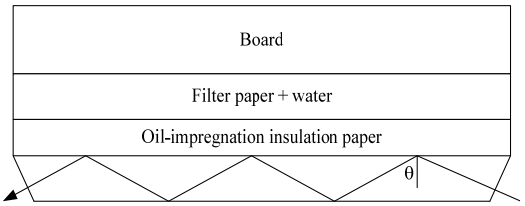

Fig. 1. Schematic description of the ATR-FTIR experimental arrangement.

2.3. 2D Correlation Analysis

For the generalized 2D correlation analysis, 20 spectra at intervals of 6 min in a wave\number range of 3000 cm^{-1} to 3700 cm^{-1} were selected. The 2D software used was a macro program named 2D-shige. In the 2D correlation maps, unshaded regions indicate positive correlation intensities, whereas shaded regions indicate negative correlation intensities. Given that the symmetric or antisymmetric relationship exists in the synchronous and asynchronous spectra, we only discussed the upper left corner area.

3. Results and Discussion

3.1. 1D Spectral Analysis

Fig. 2 shows FTIR spectra of pure water and water in oil- impregnated paper in the range of 4,000 cm^{-1} to 800 cm^{-1}. In the spectra of pure water, the bands around 3700 cm^{-1} to 3000 cm^{-1} and 1800 cm^{-1} to 1500 cm^{-1} wave number ranges are the stretching ν(OH) and deformation vibration bands δ(OH) of water, respectively. In the spectra of the mineral and vegetable oil-impregnated paper after moisture absorption, the stretching band and deformation vibration bands were evident in the 3700 cm^{-1} to 3000 cm^{-1} and the 1800 cm^{-1} to 1500 cm^{-1} regions. The ν(OH) absorption peak in pure water and hygroscopic oil- impregnated paper located at 3378 and 3335 cm^{-1}, respectively. Compared with pure water, the ν(OH) absorption band peak in oil-impregnated paper move to the lower wave number of 43 cm^{-1}. Compared with the strong intensity of the ν(OH) absorption band, the δ(OH) band is relatively weak and does not vary very significantly.

The time-evolved spectra for water diffusion in two types of oil-impregnated paper within the range of 3700 cm^{-1} to 3000 cm^{-1} are shown in Fig. 3. The absorption peaks gradually increased with time as water diffused into oil-impregnated paper. The

absorption peaks at the two kinds of oil- impregnated paper were located at 3335 cm^{-1}.

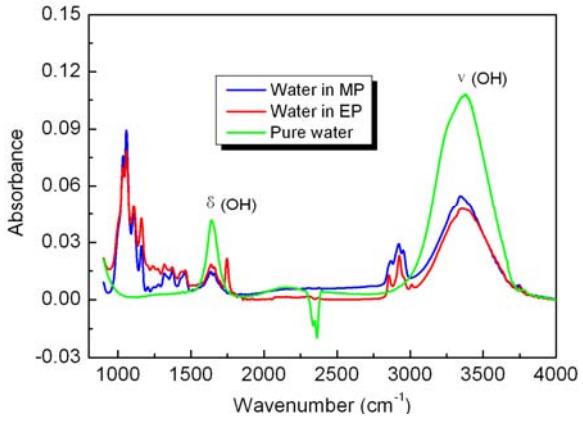

Fig. 2. ATR-FTIR spectra of absorbed water in oil-impregnated insulation paper.

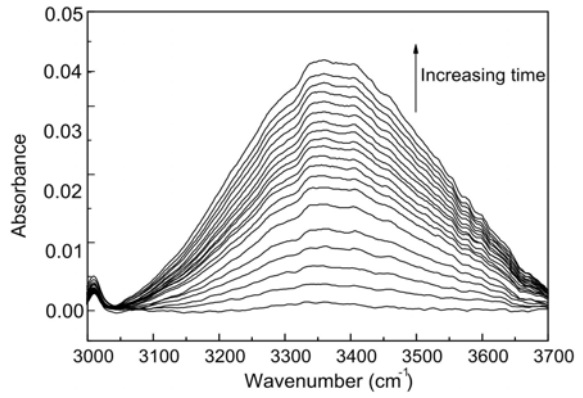

(a)

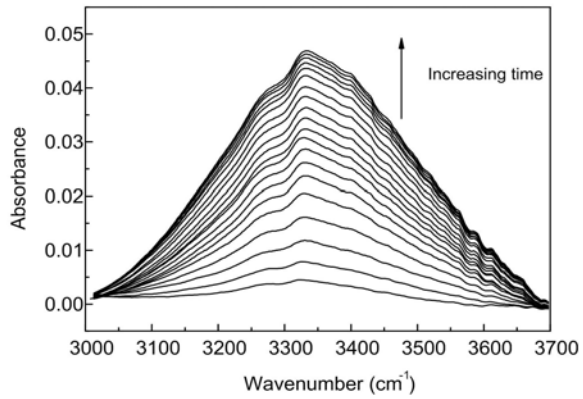

(b)

Fig. 3. ATR-FTIR spectra of absorbed water in oil paper as fluctuation of time: (a) Vegetable oil-impregnated paper; (b) Mineral oil-impregnated paper.

3.2. Two-dimensional Correlation Analysis

The generalized 2D correlation spectroscopy is used to evaluate various kinds of fluctuating perturbations, including temperature, pressure, and concentration, or any other physical variable. This tool provides more detailed information and insights into molecular interactions by correlating the absorption band intensities of different functional groups.

Two kinds of correlation maps were used, namely, synchronous and asynchronous spectra, which are generated based on a set of dynamic spectra. In the 2D synchronous spectra, the synchronous spectrum is symmetric about the leading diagonal position. In the 2D correlation map, two kinds of peaks Φ (ν1, ν2) are present, namely, auto-peak and cross-peak. The auto-peak is located in the leading diagonal position (ν1=ν2), which represents the sensitivity of absorption bands to a certain perturbation effect. The cross-peak is located in the non-leading diagonal position, which represents the same or different changes in the two peaks.

The synchronous correlation spectra of both vegetable and mineral oil-impregnated paper in the spectral range of 3700 cm^{-1} to 3100 cm^{-1} are shown in Fig. 4. One auto-peak was observed at about 3380 cm^{-1} in Fig. 4(a), which represents the OH stretching vibration. The auto-peak indicates that the OH absorption peak gradually changed during water diffusion. The same information can also be shown in Fig. 4(b). Moreover, a larger auto-peak at 3360 cm^{-1} was observed.

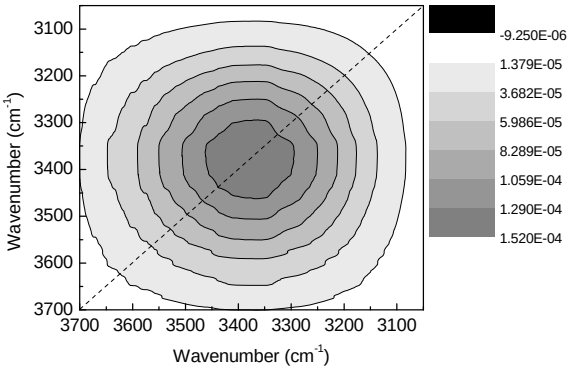

(a)

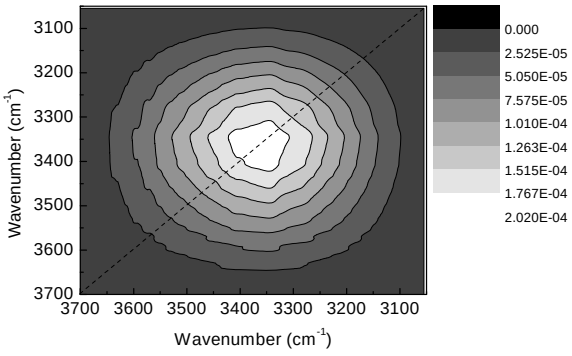

(b)

Fig. 4. Synchronous 2D correlation spectra: (a) Vegetable oil; (b) mineral oil.

More information can be obtained from the corresponding asynchronous correlation spectrum of both vegetable and mineral oil-impregnated paper in Fig. 5. An asynchronous cross-peak φ (ν1, ν2) indicates that the bands ν1 and ν2 varied out of phase with each other according to the Noda rule [7]. If φ (ν1, ν2) > 0, Φ(ν1, ν2) is positive (unshaded area), band ν1 varies before band ν2. If Φ(ν1, ν2) is negative (shaded area), implies the opposite phenomena, which is band ν1 varies after band ν2 does. If φ (ν1, ν2) < 0, this rule is reversed. In the upper left triangle of Fig. 5(a), two positive cross-peaks (3413, 3198, 3335, and 3198 cm^{-1}) dominate the asynchronous map, which indicates the broad ν(OH) water band in the spectral region of 3700 cm^{-1} to 3100 cm^{-1} is split into three separate bands located at 3425, 3357 and 3216 cm^{-1}. In addition, this result shows that during water diffusion, the band at 3425 and 3357 cm^{-1} changed prior to the band at 3216 cm^{-1}.

Similarly, in Fig. 5(b), one positive cross-peak (3346, 3216 cm-1) and two negative cross-peaks (3628, 3346 cm-1, 3425, and 3346 cm^{-1}) were observed in the upper left triangle, which indicates that the broad water band in the spectral range of 3700 cm-1 - 3100 cm^{-1} is composed of four separate bands located at 3628, 3425, 3346 and 3216 cm^{-1}. During water absorption, the band at 3346 cm^{-1} varies prior to the band at 3216 cm^{-1} and the band at 3628 and 3425 cm^{-1} changes after 3216 cm^{-1}.

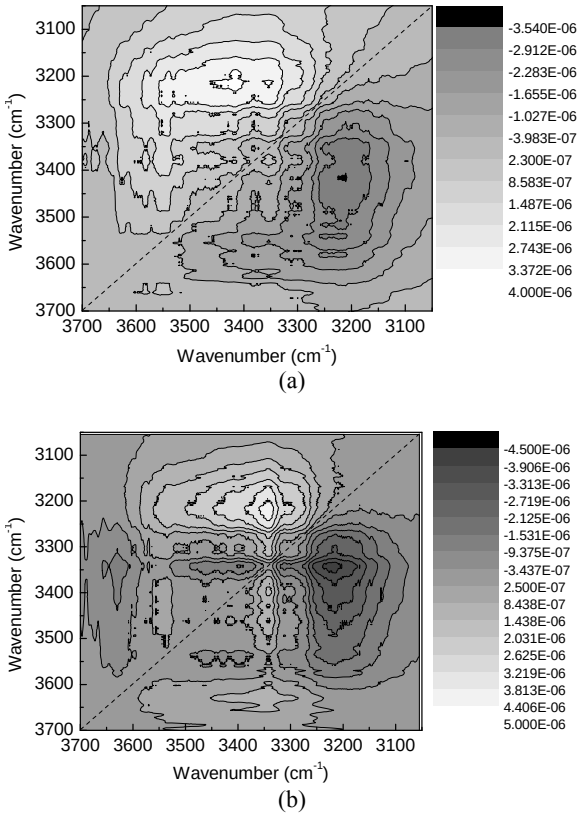

Fig. 5. Asynchronous correlation spectrum of vegetable and mineral oil-impregnated paper.

The 3425, 3346, and 3216 cm^{-1} bands express the symmetric and asymmetric stretching vibration absorption peaks of the hydroxyl of strong hydrogen bonds between water molecules. The 3628 cm^{-1} band expresses the symmetric and asymmetric stretching vibration absorption peak of the hydroxyl of weak hydrogen bonds between water molecules and the hydrophilic group of the insulating paper. Moreover, the 3346 cm^{-1} intensity changed before 3628 cm^{-1} according to the Noda rule. This result indicated that water in the form of molecules diffused into the mineral oil-immersed insulating paper, and formed hydrogen bonds with hydrophilic groups in the insulating paper. However, in the vegetable oil-immersed insulating paper, this phenomenon is not very obvious.

3.3. Diffusion Characteristics

The moisture diffusion in specimens along the thickness direction can be explained by the second Fick's diffusion law in one dimension, as follows:

$$\frac{\partial C}{\partial t} = D\frac{\partial^2 C}{\partial z^2}, \tag{1}$$

where C is the moisture content in insulating paper at the location along the specimen thickness direction x at time t. D is the effective diffusion coefficient.

The solution to Equation (1) with boundary and initial conditions can be given by

$$\frac{C(z,t)}{C_0} = 1 - \frac{4}{\pi}\sum_{n=0}^{\infty}\frac{(-1)^n}{2n+1}\exp\left[\frac{D(2n+1)^2\pi^2 t}{4L^2}\right]\cos\left(\frac{(2n+1)\pi z}{2L}\right) \tag{2}$$

Based on Equation (2), the mass-transported liquid at time t compared with the equilibrium mass is given by Equation (3):

$$\frac{M_t}{M_\infty} = 1 - \sum_{n=0}^{\infty}\frac{8}{(2n+1)^2\pi^2}\exp\left[\frac{-D(2n+1)^2\pi^2 t}{4L^2}\right], \tag{3}$$

where Mt is the absorbed mass at time t, M_∞ is the equilibrium mass, and L is the oil impregnated paper thickness.

In a short time, M_t/M_∞ is very small, the Equation (3) can be simplified into Equation (4):

$$\frac{M_t}{M_\infty} = \frac{4}{L}\left(\frac{Dt}{\pi}\right)^n \tag{4}$$

In the diffusion experiment, the absorption of infrared radiation occurred at the interface between the samples (n_1) and ATR crystals (n_2). The

infrared decayed with increasing distance from the surface. The evanescent wave electric field decay can be represented as follows:

$$E = E_0 \exp(-\gamma z), \tag{5}$$

where E_0 is the electrical field strength at the surface of the ATR crystal, and γ is the penetration depth of the evanescent wave. The γ can be defined using Equation (6):

$$\gamma = \lambda / 2\pi\left(\sin^2\theta - n_{21}^2\right), \tag{6}$$

where λ is the wavelength of the infrared beam in the ATR element, θ is the incidence angle of radiation at the paper/element interface, and n_{21} is the ratio of the refractive index of oil-impregnated paper to that of the element.

Considering the convolution of the evanescent wave electric field (Equation (5)) with the diffusion profile, Equation (3) becomes:

$$\frac{A_t}{A_\infty} = 1 - \frac{8\gamma}{\pi\left[1-\exp(2L\gamma)\right]} \sum_{n=0}^{\infty} \left[\frac{\exp\left(\frac{-D(2n+1)^2\pi^2 t}{4L^2}\right)\left[\frac{(2n+1)\pi}{2L}(-\gamma 2L) + (-1)^n(2\gamma)\right]}{(2n+1)\left(4\gamma^2 + \left(\frac{(2n+1)\pi^2}{2L}\right)^2\right)} \right], \tag{7}$$

where A_t is the band absorbance of ATR-FTIR spectra at time t, and A_∞ is the band absorbance at equilibrium. The diffusion coefficient can be calculated by Equation (6).

In the 3800 cm^{-1} to 3000 cm^{-1} range, the OH absorption peak height was used as the moisture absorption amount. The functional relation between the area and time was fitted in a non-linear curve. Fitting data calculation into the program and the fitting curve was obtained, as shown in Fig. 6. The results are shown in Table 1.

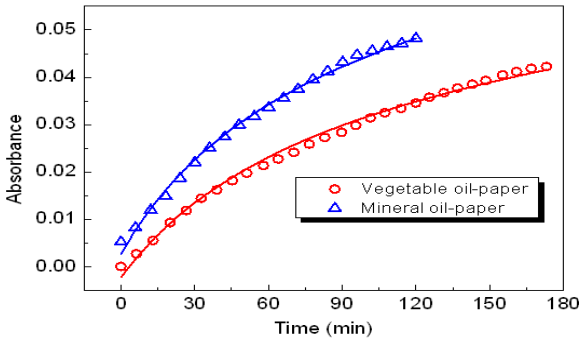

Fig. 6. Fitting curves of absorbed water in oil-paper insulation.

Table 1. Fitting results from ATR-FTIR spectra.

Parameter	M_∞	L (mm)	D (10^{-6} mm^2 s^{-1})
Mineral oil-paper	0.10711	0.3	1.5

7. Conclusions

The present work focused on the characteristics of moisture diffusion in oil-paper insulation using 2D infrared correlation spectroscopy. The experiment and analysis results are summarized as follows:

1) Based on the 2D infrared correlation analysis, water in the form of molecules diffused into the mineral oil-immersed insulating paper and formed hydrogen bonds with hydrophilic groups in the insulating paper. In vegetable oil-immersed insulating paper, this phenomenon is not very evident.

2) 2D infrared correlation analysis revealed three OH stretching vibration spectra absorption peaks in hygroscopic vegetable oil-immersed insulating paper. The peaks were 3425, 3357 and 3216 cm^{-1}, respectively. The four OH stretching vibration spectra absorption peaks in hygroscopic mineral oil-immersed insulation paper were 3425, 3346, 3216 and 3628 cm^{-1}.

3) The diffusion coefficients of water in mineral oil-immersed insulation paper and in vegetable oil-immersed insulating paper were calculated using a nonlinear curve fitting, which were 1.5×10^{-6} mm^2 s^{-1} and 1.16×10^{-6} mm^2 s^{-1}, respectively.

Acknowledgements

The authors acknowledge the National Science Foundation of China (No. 51021005 and No. 51377176). Project 111 of the Ministry of Education, China (No. B08036) is also appreciated.

References

[1]. L. E. Lundgaard, W. Hansen, D. Linhjell, *et al.*, Aging of oil-impregnated paper in power transformers, *IEEE Transactions on Power Delivery*, 19, 1, 2004, pp. 230-239.

[2]. Y. Du, M. Zahn, B. C. Lesieutre, *et al.*, Moisture equilibrium in transformer paper-oil systems, *IEEE Electrical Insulation Magazine*, 15, 1, 1999, pp. 11-20.

[3]. T. V. Oommen, Moisture equilibrium charts for transformer insulation drying practice, *IEEE Transactions on Power Apparatus and Systems,* 103, 10, 1984, pp. 3063-3067.

[4]. F. M. Clark, Factors affecting the mechanical deterioration of cellulose insulation, *Browse Journals & Magazines*, 61, 10, 1942, pp. 742-749.

[5]. A. M. Emsley, X. Xiao, R.J. Heywood, M. Ali,

Degradation of cellulosic insulation in power transformers. Part 3: Effects of oxygen and water on ageing in oil, *IEEE Proceedings: Science, Measurement and Technology*, 147, 3, 2000, pp. 115-119.

[6]. G. T. Fieldson, T. A. Barbari, The use of FTi.r.-a.t.r. spectroscopy to characterize penetrant diffusion in polymers, *Polymer*, 34, 6, 1993, pp. 1146-1153.

[7]. I. Noda, Two-dimensional infrared spectroscopy, *Journal of the American Chemical Society,* 111, 6, 1989, pp. 8116-8118.

[8]. I. Noda, Advances in two-dimensional correlation spectroscopy, *Vibration Spectroscopy*, 36, 6, 2004, pp. 143-165.

[9]. P. Wu, H. W. Siesler, Two-dimensional correlation analysis of variable-temperature Fourier-transform mid- and near-infrared spectra of polyamide 11, *Journal of Molecular Structure*, 521, 1–3, 2000, pp. 37-47.

[10]. J. Zhang, Hideto Tsuji, I. Noda, Weak intermolecular interaction during the melt crystallization of poly (L-lactide) investigated by two–dimensional infrared correlation spectroscopy, *The Journal of Physical Chemistry B*, 108, 36, 2004, pp. 11514-11520.
